Arab J Sci Eng (2014) 39:8347–8358
DOI 10.1007/s13369-014-1391-1

RESEARCH ARTICLE - PETROLEUM ENGINEERING

Experimental and Simulation Study of Complex Structure Well Pattern Optimization for Buried Hill Fractured Reservoirs

Jian Liu · Yuetian Liu · Jichang Zhang · Jie Yang · Zhengliang Guo

Received: 1 December 2013 / Accepted: 30 June 2014 / Published online: 11 October 2014

Abstract The use of a vertical well pattern results in productivity deficiency and poor development effect when developing buried hill reservoirs with complex properties. In this work, experiments are conducted to determine the best pattern for complex structure wells in buried hill reservoirs. Discretization is employed in an experimental method that uses unit cubic rocks with a size of 5 cm × 5 cm × 5 cm. The rocks are bonded in a spotty or reticular design to form a macroscopic model. Based on water flooding similarity criteria of fractured reservoir, an experimental model similar to a quarter of a five-spot unit in an actual reservoir is designed and manufactured. By selectively plugging wells in the model, various well patterns are established. Simulation results indicate that the vertical–vertical well pattern exhibits the fastest water breakthrough, fastest increase in water cut, and lowest recovery under the same pressure difference and well spacing. The horizontal–horizontal well pattern has the slowest water cut increase and the highest final oil recovery. For fishbone wells, this pattern facilitates an ideal development effect when the percolation direction is perpendicular to the plane determined by the mother bore and branch. When liquid rate, water cut, and recovery are considered, the horizontal–horizontal well pattern is recommended when conditions allow.

J. Liu (✉) · Y. Liu · Z. Guo
MOE Key Laboratory of Petroleum Engineering
in China University of Petroleum, Beijing 102249, China
e-mail: kevenlj@163.com

J. Liu
Research Institute of Petroleum Exploration and Development,
Beijing 100083, China

J. Zhang · J. Yang
Shenyang Oil Plant of Liaohe Oilfield, Shenyang 110316, China

Keywords Fracture · Discretization · Similarity · Well pattern · Development effect

الخلاصة

إن استخدام نمط البئر العمودي ينتج نقصا في الإنتاجية وفقرا في تأثير التنمية عند تطوير خزانات تلة مدفونة مع خصائص معقدة. وقد أجريت -في هذا العمل -التجارب لتحديد أفضل نمط للآبار ذات البنية المعقدة في خزانات التلة المدفونة. وتم تطبيق التفريد في الأسلوب التجريبي الذي يستخدم وحدة صخور مكعبة بحجم 5 سم × 5 سم × 5 سم. وربطت الصخور في تصميم متقطع أو شبكي لتشكيل النموذج العياني. وبناء على معايير تشابه فيضانات المياه من خزان مكسور تم تصميم نموذج تجريبي مماثل لربع وحدة من خمس بقع في الخزان الفعلي وتصنيعها. وتم من خلال التوصيل الانتقائي للآبار في النموذج تأسيس أنماط آبار مختلفة. وتُشير نتائج المحاكاة إلى أن نمط البئر العمودي - العمودي يظهر أسرع اختراق للمياه ، وأسرع زيادة في قطع المياه ، وأدنى استخراج تحت نفس فرق الضغط وتباعد البئر. ولنمط البئر الأفقي - الأفقي أبطأ زيادة قطع مياه وأعلى استخراج نفط نهائي. وللآبار الحسكية ، هذا النمط يسهل من تأثير التطور المثالي عندما يكون اتجاه الترشيح عموديا على المستوى المحدد من قبل الثقب الأم والفرع. عندما تؤخذ سرعة السائل ، وقطع المياه ، والاستخراج في الاعتبار يوصى بنمط البئر الأفقي - الأفقي عندما تسمح الظروف بذلك.

1 Introduction

The complex structure well technique that was developed in the twentieth century can reduce water and gas coning, improve the production of thin and fractured reservoirs, and contribute to higher oil and gas production while producing lower cost and greater economic benefit, especially in cases in which vertical wells are not economical.

Complex structure wells can generally be categorized into horizontal, fishbone, and multilateral wells. The benefit from the increase in production provided by a horizontal well is usually greater than the cost of drilling the horizontal

section. Horizontal wells have been widely used by reservoir engineers since the end of the 1980s [1]. Fishbone well technology extends the horizontal section plane with a single horizontal wellbore to a plane with more than one horizontal wellbore, achieving a more exposed reservoir area and increasing well production [2]. Multilateral well technology improves well productivity by maximizing reservoir contact, resulting in a development with fewer wells while minimizing water and gas coning [3]. Multilateral well technology has been applied to increase the production rate per well [4].

1.1 Theoretical Research

As complex structure well technology became widely applied in oilfield development, an increasing number of theories and technologies have been developed for such wells. Mathematical models for multilateral well productivity prediction have been presented and modified [5–10], and parameters for the optimization of complex structure wells have been studied [11–13].

1.2 Application

Multilateral and fishbone wells have been applied in countries in the Middle East and South America, including the UAE, Saudi Arabia, Oman, Iran, Qatar, Kuwait, Bahrain, Iraq, and Venezuela [14,15]. For example, Saudi Aramco has drilled over 440 horizontal and maximum reservoir contact wells since 2002.

Building complex structure wells is an effective approach for economic development. Such reservoirs are characterized by low permeability, low abundance, bottom water, heavy oil, ultra-thinness, multilayer, coalbed methane, and natural gas reservoir [16,17]. Complex structure well technology has also been widely used recently for the development of buried hill reservoirs.

(a) Low-Permeability Reservoir

Hao [18] presented a new method that couples non-Darcy elliptical and Darcy radial flows to the horizontal wellbore in fractured reservoirs to predict and optimize the productivity of multiple transverse fractured horizontal wells in ultra-low- permeability reservoirs. Yu [19] compared the difference between the development effects of low-permeability reservoir in multi-fractured horizontal wells and that in fishbone wells. Bigno [20] studied horizontal and multilateral well technology to develop low-permeability reservoirs.

(b) Bottom Water Reservoir

Zhou [21] studied horizontal well water flooding performance and its influencing factors and was the first to illustrate the water flooding patterns of horizontal wells in bottom water reservoir.

(c) Heavy-Oil Reservoirs

Horizontal and multilateral wells are designed to develop heavy-oil reservoirs because of the advantages of these wells in terms of enhanced oil recovery [3,22].

(d) Ultra-Thin Reservoir

Two fishbone wells have been drilled in the reservoir of which the thickness is 1.5 m in Daqing oilfield that is currently the thinnest reservoir with fishbone wells, and many technical problems arising from drilling in an ultra-thin oil layer have been solved successfully [2,23].

(e) Multilayer Reservoir

A semi-analytical model of multilateral well was presented by Yan [24]. This model can predict the production performance of a complex structure well in multilayer reservoirs with different porosities and anisotropic permeabilities, obtain information about reservoir connectivity, and estimate well and reservoir properties in a multilayer system.

(f) Coalbed Methane Reservoirs

Maricic [25] compared the drilling cost of dual-, tri-, and quad-laterals with fishbone wells and studied the total length of horizontal wells, as well as the distance between laterals in these configurations.

(g) Gas-Drive Reservoir

Rivera [26] established multilateral well technologies, analyzed the application of multilateral well technology in reservoirs, and suggested that the behavior of multilateral wells is similar to the solution gas-drive mechanism.

(h) Buried Hill Reservoir

The buried hill reservoirs are in fact remnant topography (irregular unconformity surfaces) that has been buried beneath younger sediments. Many of the onshore Chinese basins contain buried hill reservoirs [27]. The application of multilateral wells in buried hill reservoirs achieved satisfactory development performance. Such application has become a common approach to the development of similar reservoirs because of the significant economic benefit provided by multilateral wells [28]. A buried hill reservoir features developed fractures, good connection, and thick layer [29], resulting in low productivity and poor development effect when developed with vertical wells. Given the problems existing in developing reservoirs with vertical wells, considerable research has been conducted on the mechanisms of complex structure wells, parameters for optimizing stereo injection–production, productivity, and influencing factors of the development of horizontal wells [30–35]. The well pattern of vertical and horizontal wells was proposed, which contributed to the improvement of buried hill reservoir development.

This paper reports on the best well pattern and development law for buried hill reservoirs through experiments. The fabrication method of the experimental model and wellbore presetting are proposed. Based on the target reservoir, a similar experimental model is established with different well pat-

terns, through which water flooding experiments can be conducted to examine the development effect. Combined with the development effect, the best complex structure well pattern is determined to provide theoretical and technical support for the further enhancement of oil recovery.

2 Fabrication Method of Experimental Model

2.1 Principle of Model Fabrication

A fractured reservoir consists of a fracture system and a matrix system. A vertically crossed fracture network (as shown in Fig. 1) can represent the distribution of actual fractures.

By discretization, the experimental model is established by adhering cubic blocks with size of 5 cm × 5 cm × 5 cm fabricated by crude outcropping sand. The bonded face between blocks adhered by points indicates a fracture, whereas a reticulate indicates an inactive fracture. Fracture properties, such as permeability and porosity, can be controlled quantitatively by adjusting fracture density.

The width of fracture is affected by manufacturing precision of unit blocks and the volume of binder. To control the fracture width, firstly, we must be sure that the manufacturing precision of the unit blocks is precise enough. The outcrop rocks are made into cubic blocks with the size of 50 mm by infrared automatic cutting machine, and the error of the size is less than 1 % after the selection of using vernier caliper. Based on the strict precision control of unit blocks manufacturing and selection, all the sizes of the unit blocks are equal with each other, and therefore, the fracture surfaces are parallel and then control the volume of binder strictly. The depth of binder penetrates into the unit blocks are limited and equal due to high viscosity of binder and low permeability of matrix. The volume of binder is controlled precisely by dispenser, so that the thicknesses of binder between the two bonded surfaces are the same. As a result, the widths of fractures are the same when the precision of unit blocks manufacturing and the volume of binder are controlled.

2.2 Design of Fracture System

A Cartesian coordinate system (x, y, z) is established with three axes parallel to the three principal directions of anisotropic permeability. The fracture permeability at each direction is supposed to be K_x, K_y, K_z, whereas the fracture density perpendicular to each direction is N_x, N_y, N_z, respectively. The formulas of fracture permeability are [36]

$$\bar{K}_{ex} = N_x k \begin{bmatrix} 0 & 0 & 0 \\ 0 & 1 & 0 \\ 0 & 0 & 1 \end{bmatrix}, \bar{K}_{ey} = N_y k \begin{bmatrix} 1 & 0 & 0 \\ 0 & 0 & 0 \\ 0 & 0 & 1 \end{bmatrix},$$
$$\bar{K}_{ez} = N_z k \begin{bmatrix} 1 & 0 & 0 \\ 0 & 1 & 0 \\ 0 & 0 & 0 \end{bmatrix} \quad (1)$$

The total anisotropic permeability in this fracture system is given by Eq. (2)

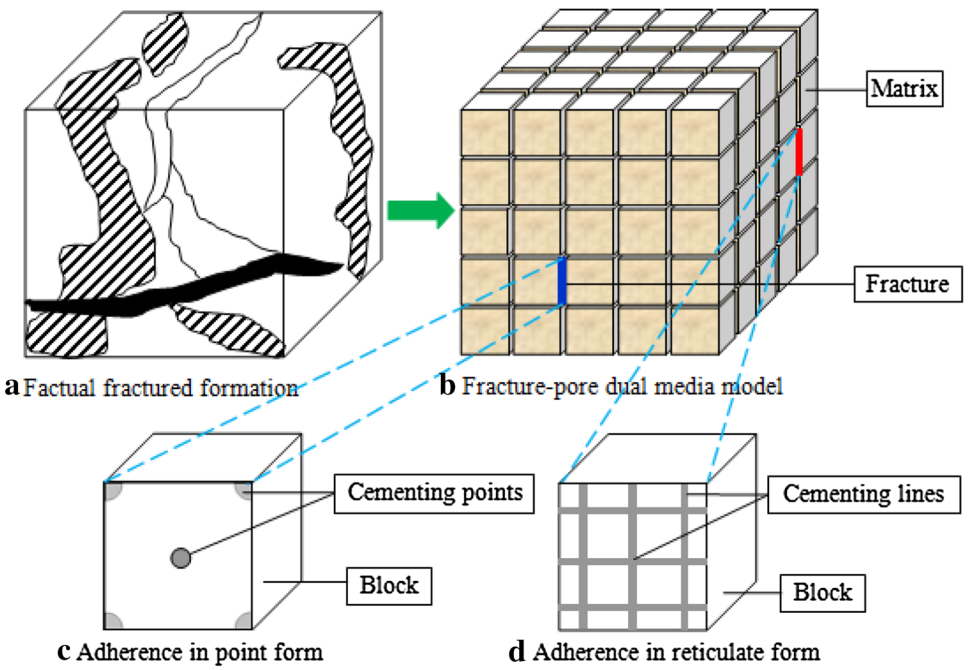

Fig. 1 Structure of dual porous media

$$\bar{K}_e = \bar{K}_{ex} + \bar{K}_{ey} + \bar{K}_{ez} = k \begin{bmatrix} N_y + N_z & 0 & 0 \\ 0 & N_x + N_z & 0 \\ 0 & 0 & N_x + N_y \end{bmatrix} \quad (2)$$

The ratio among principal values of permeability at each direction is

$$k_x : k_y : k_z = \left(N_y + N_z\right) : (N_x + N_z) : \left(N_x + N_y\right) \quad (3)$$

This ratio can be transformed as

$$N_x : N_y : N_z = (k_y + k_z - k_x) : (k_z + k_x - k_y) : (k_x + k_y - k_z) \quad (4)$$

Formula (4) represents the condition of fracture distribution, considering the anisotropy of permeability.

2.3 Realization of Wellbore and Well Pattern Combination

2.3.1 Method for Wellbore Presetting

A wellbore is discretized into segments by drilling wellbores in cubic blocks and then adhering them to form the entire wellbore, as shown in Fig. 2. Hence, different wells, including vertical, horizontal, and fishbone wells, can be preset within the model.

2.3.2 Plugging of Preset Wellbore

Elastic pipelines, which are expandable and retractable with pressure variation, are placed in the wellbore. The fluid pressure in elastic pipelines is controlled by an external pressure source to achieve plugging and unblocking, as shown in Fig. 3. By selectively plugging wellbores in the model, the target well pattern can be realized.

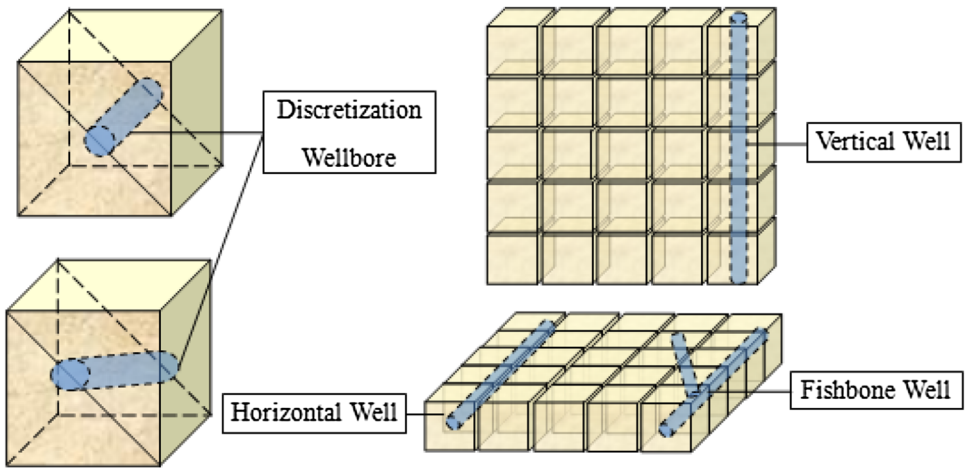

Fig. 2 Diagram of presetted wellbore

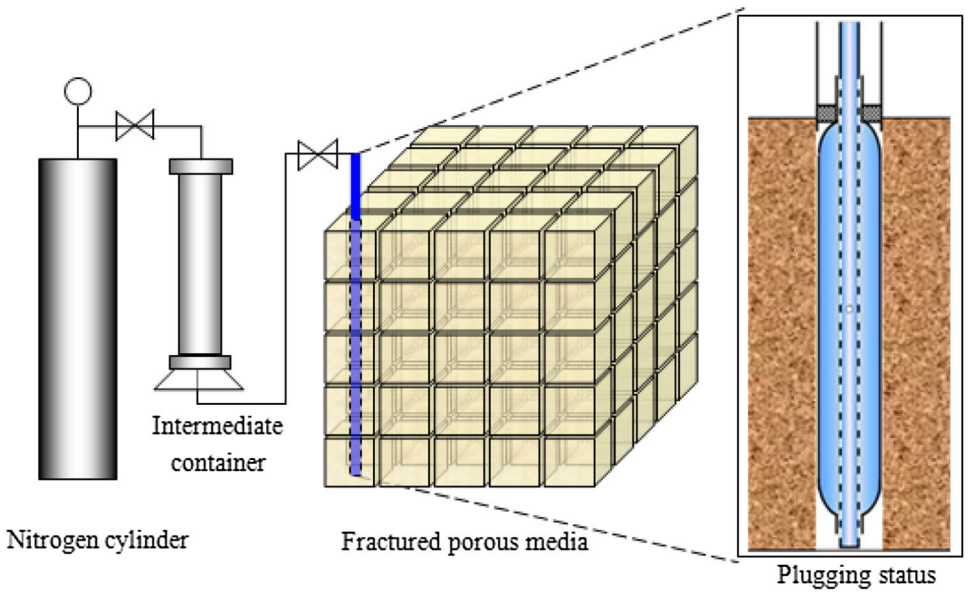

Fig. 3 Plugging of presetted wellbore

3 Similarity Principle of Fractured Reservoir

The experimental conditions for water flooding in fractured reservoir are assumed as follows [34]: (1) The reservoir media are characterized by dual porosity and single permeability with matrix and fractures for fluid storage and a fracture system as a percolation channel; (2) imbibition exists between the matrix and fractures, and capillary pressure within fractures is ignored; (3) the influence of oil–water gravity difference is considered; (4) rock media and fracture permeability are anisotropic; and (5) compressibility of fluid and rock is neglected.

3.1 Mathematical Model

The motion equations for the fracture system are given by

$$\begin{cases} \text{water}: \quad \vec{v}_{\mathrm{w}} = -\mathbf{A_w} \cdot \nabla \Phi_{\mathrm{w}} \\ \text{oil}: \quad \vec{v}_{\mathrm{o}} = -\mathbf{A_o} \cdot \nabla \Phi_{\mathrm{o}} \end{cases} \tag{5}$$

where $\vec{v}$ is flow velocity and the subscripts o, w denote oil and water, respectively. $\mathbf{A_w}$ and $\mathbf{A_o}$ are the tensors of water and oil mobility, respectively, and are formulated as

$$\mathbf{A_o} = \frac{\mathbf{K}K_{\mathrm{ro}}}{\mu_{\mathrm{o}}}, \qquad \mathbf{A_w} = \frac{\mathbf{K}K_{\mathrm{rw}}}{\mu_{\mathrm{w}}} \tag{6}$$

$\mathbf{K}$ is the tensor of anisotropic permeability. K_{ro} and K_{rw} are the relative permeabilities of oil and water, respectively. μ_{o} and μ_{w} are the velocities of oil and water, respectively. Φ_{o} and Φ_{w} are potentials of the oil and water phases, respectively, and are formulated as

$$\Phi_{\mathrm{o}} = p + \gamma_{\mathrm{o}} D, \qquad \Phi_{\mathrm{w}} = p + \gamma_{\mathrm{w}} D \tag{7}$$

where p is pressure, γ is specific gravity, and D is depth.

The material balance equations for the fracture system are

$$\begin{cases} \text{water}: \quad \nabla \cdot \vec{v}_{\mathrm{w}} - q_{\mathrm{w}} = -\Phi \frac{\partial S_{\mathrm{w}}}{\partial t} \\ \text{oil}: \quad \nabla \cdot \vec{v}_{\mathrm{o}} - q_{\mathrm{o}} = -\Phi \frac{\partial S_{\mathrm{o}}}{\partial t} \end{cases} \tag{8}$$

where q and S are imbibition rate and saturation, respectively, and Φ is the porosity.

The imbibition equation between matrix and fracture is formulated as

$$\begin{aligned} q_{\mathrm{o}} &= R \cdot \frac{\ln 2}{T_{\mathrm{a}}} \left[S_{\mathrm{w}}(x, y, z, t) \right. \\ &\quad \left. - \frac{\ln 2}{T_{\mathrm{a}}} \int_0^t S_{\mathrm{w}}(x, y, z, \tau)\, \mathrm{e}^{\frac{\ln 2}{T_{\mathrm{a}}}(\tau - t)} \mathrm{d}\tau \right] \\ &= R \cdot \frac{\ln 2}{T_{\mathrm{a}}} \int_0^t \frac{\partial S_{\mathrm{w}}}{\partial \tau} \cdot \mathrm{e}^{\frac{\ln 2}{T_{\mathrm{a}}}(\tau - t)} \mathrm{d}\tau \end{aligned} \tag{9}$$

where R is the movable oil volume per unit matrix volume; T_{a} is the half-cycle of imbibition; t is time; τ is the intermediate variable; and x, y, z are the coordinates in rectangular space of the reservoir.

The formulas for relative permeability equations of oil and water, without considering the capillary for fracture, are given by

$$K_{\mathrm{rw}} = S_{\mathrm{w}}, \quad K_{\mathrm{ro}} = 1 - S_{\mathrm{w}} \tag{10}$$

The naturally satisfied equations are

$$S_{\mathrm{o}} + S_{\mathrm{w}} = 1, \quad q_{\mathrm{w}} + q_{\mathrm{o}} = 0 \tag{11}$$

The initial conditions are

$$\begin{aligned} &\Phi_{\mathrm{o}}(x, y, z, t = 0) = \Phi_i, \quad \Phi_{\mathrm{w}}(x, y, z, t = 0) = 0, \\ &S_{\mathrm{w}}(x, y, z, t = 0) = 0 \end{aligned} \tag{12}$$

where Φ_i is the initial potential distribution.

Boundary conditions: reservoir boundary Γ is a closed boundary with a normal boundary n,

$$\left.\frac{\partial \Phi_{\mathrm{o}}}{\partial n}\right|_{\Gamma} = 0, \quad \left.\frac{\partial \Phi_{\mathrm{w}}}{\partial n}\right|_{\Gamma} = 0 \tag{13}$$

A wellbore is assumed to have fixed injection–production pressure difference, formulated as

$$p\left(\vec{r}_{\mathrm{inj}}, t\right) - p\left(\vec{r}_{\mathrm{pro}}, t\right) = \Delta p \tag{14}$$

where r_{w} is the wellbore radius; $\vec{r}_{\mathrm{inj}} = (x, y, z)_{\mathrm{inj}}$ and $\vec{r}_{\mathrm{pro}} = (x, y, z)_{\mathrm{pro}}$ are the vector coordinates on the injection and production wellbore, respectively; and Δp is injection and production differential pressure.

Combining Eqs. (5)–(14), the water flooding mathematical model of fractured reservoir can be expressed by Eq. (15).

$$\begin{cases} \frac{\partial}{\partial x}\left[\left(K_x \cdot (1 - S_{\mathrm{w}}) + \frac{\mu_{\mathrm{o}}}{\mu_{\mathrm{w}}} \cdot K_x S_{\mathrm{w}}\right) \cdot \frac{\partial \Phi_{\mathrm{w}}}{\partial x}\right] \\ \quad + \frac{\partial}{\partial y}\left[\left(K_y \cdot (1 - S_{\mathrm{w}}) + \frac{\mu_{\mathrm{o}}}{\mu_{\mathrm{w}}} \cdot K_y S_{\mathrm{w}}\right) \cdot \frac{\partial \Phi_{\mathrm{w}}}{\partial y}\right] \\ \quad + \frac{\partial}{\partial z}\left[\left(K_z \cdot (1 - S_{\mathrm{w}}) + \frac{\mu_{\mathrm{o}}}{\mu_{\mathrm{w}}} \cdot K_z S_{\mathrm{w}}\right) \cdot \frac{\partial \Phi_{\mathrm{w}}}{\partial z}\right] \\ \quad - \frac{\partial}{\partial z}\left[K_z \cdot (1 - S_{\mathrm{w}})\, \Delta\gamma\right] = 0 \\ \frac{\partial}{\partial x}\left[\frac{K_x \cdot S_{\mathrm{w}}}{\mu_{\mathrm{w}}} \cdot \frac{\partial (\Phi_{\mathrm{o}} - \Phi_i)}{\partial x}\right] + \frac{\partial}{\partial y}\left[\frac{K_y \cdot S_{\mathrm{w}}}{\mu_{\mathrm{w}}} \cdot \frac{\partial (\Phi_{\mathrm{o}} - \Phi_i)}{\partial y}\right] \\ \quad + \frac{\partial}{\partial z}\left[\frac{K_z \cdot S_{\mathrm{w}}}{\mu_{\mathrm{w}}} \cdot \frac{\partial (\Phi_{\mathrm{o}} - \Phi_i)}{\partial z}\right] \\ \quad + \frac{\partial}{\partial z}\left(\frac{K_z \cdot S_{\mathrm{w}}}{\mu_{\mathrm{w}}} \cdot \Delta\gamma\right) - R\frac{\ln 2}{T_{\mathrm{a}}} \int_0^t \frac{\partial S_{\mathrm{w}}}{\partial \tau} \cdot \mathrm{e}^{-\frac{\ln 2}{T_{\mathrm{a}}}(t - \tau)} \mathrm{d}\tau = \Phi \cdot \frac{\partial S_{\mathrm{w}}}{\partial t} \\ \Phi_{\mathrm{o}}(x, y, z, 0) - \Phi_i = 0, \quad \Phi_{\mathrm{w}}(x, y, z, 0) = 0 \\ S_{\mathrm{w}}(x, y, z, 0) = 0 \\ \left.\frac{\partial \Phi_{\mathrm{o}}}{\partial n}\right|_{\Gamma} = 0, \quad \left.\frac{\partial \Phi_{\mathrm{w}}}{\partial n}\right|_{\Gamma} = 0 \\ p\left(\vec{r}_{\mathrm{inj}}, t\right) - p\left(\vec{r}_{\mathrm{pro}}, t\right) = \Delta p \end{cases} \tag{15}$$

Table 1 Similarity criterion for simulation of water flooding in fractured anisotropic reservoir

Similarity	Expressions	Definitions	Effects
π_1	L_x/L_y	Ratio of characteristic length in x direction to characteristic length in y direction	Similarity of size
π_2	L_x/L_z	Ratio of characteristic length in x direction to characteristic length in z direction	
π_3	x/L_x	Dimensionless x coordinate	Similarity of shape and space
π_4	y/L_y	Dimensionless y coordinate	
π_5	z/L_z	Dimensionless z coordinate	
π_6	$\bar{K}_y/\bar{K}_x$	Ratio of permeability in y direction to permeability in x direction	Similarity of anisotropy of permeability
π_7	$\bar{K}_z/\bar{K}_x$	Ratio of permeability in z direction to permeability in x direction	
π_8	$K_x/\bar{K}_x$	Dimensionless permeability in x direction	Similarity of heterogeneity of permeability
π_9	$K_y/\bar{K}_y$	Dimensionless permeability in y direction	
π_{10}	$K_z/\bar{K}_z$	Dimensionless permeability in z direction	
π_{11}	$\Phi/\bar{\Phi}$	Dimensionless porosity	Similarity of heterogeneity of permeability
π_{12}	r_w/L_x	Ratio of well radius to characteristic length	Similarity of wellbore geometry parameters
π_{13}	$\bar{\mu}_o/\bar{\mu}_w$	Ratio of oil–water viscosity	Similarity of viscous resistance of fluid flow
π_{14}	$L_z \cdot \Delta\bar{\gamma}/\Delta p$	Ratio of gravitational pressure difference to injection–production pressure difference	Similarity of dynamics
π_{15}	$\bar{R}/\bar{\Phi}$	Ratio of movable oil in matrix to movable oil in fractures	Similarity of reserves of matrix and fracture
π_{16}	$R/\bar{R}$	Dimensionless movable oil volume per unit matrix volume	Similarity of relation between imbibition and flooding
π_{17}	$\bar{T}^*/T$	Ratio of characteristic time of imbibition to characteristic time of flooding	Similarity of relation between imbibition and flooding
π_{18}	$T^*/\bar{T}^*$	Dimensionless half-cycle of imbibition	Similarity of imbibition strength distribution
π_{19}	t/T	Dimensionless time	Similarity of time and process
π_{20}	$\Phi_w/\Delta p$	Dimensionless water potential	Similarity of potential distribution
π_{21}	$(\Phi_o - \Phi_i)/\Delta p$	Dimensionless oil potential	
π_{22}	S_w	Dimensionless water	Similarity of saturation distribution

3.2 Similarity Criteria

Based on dimensional analysis and similarity principle [29, 35], a similarity criterion system is established. This system consists of 22 similarity criteria, as listed in Table 1.

4 Water Flooding Experiment

4.1 Background of Factual Reservoir

A fractured buried hill reservoir in Liaohe oilfield develops three groups of structural fractures, i.e., NE–NNE direction, NW direction, and approximately EW direction with permeabilities of $K_1 = 360.8 \times 10^{-3}\,\mu\text{m}^2$, $K_2 = 213.3 \times 10^{-3}\,\mu\text{m}^2$, and $K_3 = 80.5 \times 10^{-3}\,\mu\text{m}^2$, respectively. Among the fractures, mid–high-angle fractures (70°–90°) account for 32 %, oblique fractures (20°–70°) account for 58.4 %, and low-angle fracture (<20°) account for 9.6 %. A 1/4 unit of stereo five-spot well pattern in the target reservoir is selected to identify the best well pattern. Based on water flooding similarity criteria of the fractured reservoir, the experimental model is fabricated with vertical, horizontal, and fishbone wells. The development effect of different well patterns can be revealed by water flooding experiments.

4.2 Distribution of Fractures

According to the calculation method of permeability anisotropy [37], the ratio of anisotropic permeability in the X, Y, Z direction is given by

$$K_x : K_y : K_z = 1 : 1.05 : 1.4 \tag{16}$$

Combining Eqs. (4) and (16), the number of fractures perpendicular to the X, Y, Z directions are 10, 9, and 9, respectively. In practice, every bonded face perpendicular to the X direction makes a fracture, which is the maximum fracture density in the model, whereas one fracture is made for

every two bonded faces perpendicular to the Z direction. The first, second, third, fourth, fifth, sixth, eighth, ninth, and tenth bonded faces perpendicular to the Y direction are chosen to make nine fractures.

4.3 Design of Well Patterns

According to the similarity criteria, six wells are preset in the model, with Z1 and Z2 as vertical wells, S1 and S2 as horizontal wells, and Y1 and Y2 as fishbone wells with a single branch 30 cm long at a 25° angle [intersection point of branches with main boreholes are (4, 11, 21) and (8, 1, 11), respectively]. The wells preset within the model are shown in Fig. 4.

Based on the objective of this research, the method mentioned in Sect. 2.3 is used to design five experimental schemes with the details shown in Table 2. Experiments are conducted under atmospheric temperature with a constant pressure difference of 0.27 m water column. The liquid production, water production, and the corresponding time are recorded, and the water cut is calculated. The experiment was terminated when the water cut reached 100 %.

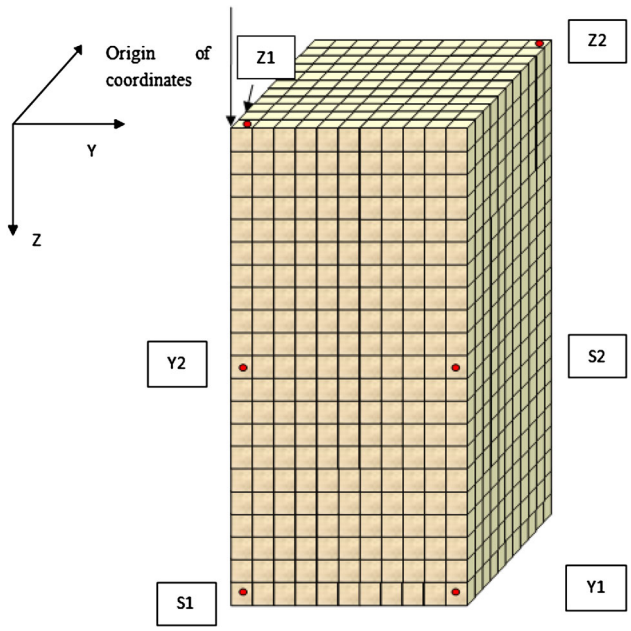

Fig. 4 Outline of wells presetted within the experimental model

4.4 Processing and Selection of Rocks

After nearly eight months of trial and selection, sandstone outcrops are selected and transported from the provinces of Hebei, Shanxi, Yunnan, and Sichuan. More than 300 core test experiments are conducted, and natural yellow sandstones are selected as the model-making materials. A total of 3,500 blocks, with a size error of less than 0.1 mm and an angle error of less than 0.5°, are selected from 6,000 cube blocks, which are processed from natural sandstone outcrops with a size of 5 cm × 5 cm × 5 cm.

4.5 Establishment of Similarity Experimental Model

Two bonding methods are combined to establish the model with a developed high-angle fracture. Based on an actual buried hill reservoir in Liaohe oilfield, an experimental model with cubic blocks of $11 \times 11 \times 21 = 2{,}541$ is established according to the principle in Sect. 2.1. The manufacturing process is shown in Fig. 5. The length of a unit cubic block is 5 cm, the size of the model is 55 cm × 55 cm × 105 cm, and the fracture width is proximately 0.02 cm, as shown in Fig. 6. A PVC pipe with 6 mm outer diameter and 4 mm inner diameter is selected for the wellbore, and one with an outer diameter of 4 mm and an inner diameter of 2.5 mm is selected for the pressure pipeline. A wellbore is a barefoot well completion, and simulated oil with a viscosity of 14.48 mPa s and water with a viscosity of 1 mPa s are selected as experimental fluids. The macroscopic model is shown in Fig. 7.

The parameters of target reservoir and experimental model are listed in Table 3. The compositions of injected water are as shown in Table 4. Hydrocarbon, wax, resin, and asphaltene contents in crude oil are 52.03, 34.23, and 13.74 %, respectively.

5 Analysis and Discussions

5.1 Comparison with Numerical Simulation

The numerical model is established using eclipse. Cartesian coordinates, block center grid, black oil simulator, and laboratory units are selected to establish a dual porosity single

Table 2 Experiment design for different cases

No. of cases	Well pattern	Well	Remark
Case 1	Vertical well–fishbone well	Z1, Z2	Z1 for injection, Z1 for production
Case 2	Fishbone well–fishbone well	Y1, Y2	Y1 for injection, Y2 for production
Case 3	Horizontal well–fishbone well	S1′, Y2	S1′ for injection, Y2 for production
Case 4	Fishbone well–horizontal well	Y1, S2′	Y1 for injection, S2′ for production
Case 5	Horizontal well–horizontal well	S1, S2	S1 for injection, S2 for production

Horizontal well S2′ is well Y2 with its branch plugged, and horizontal well S1′ is well Y1 with its branch plugged

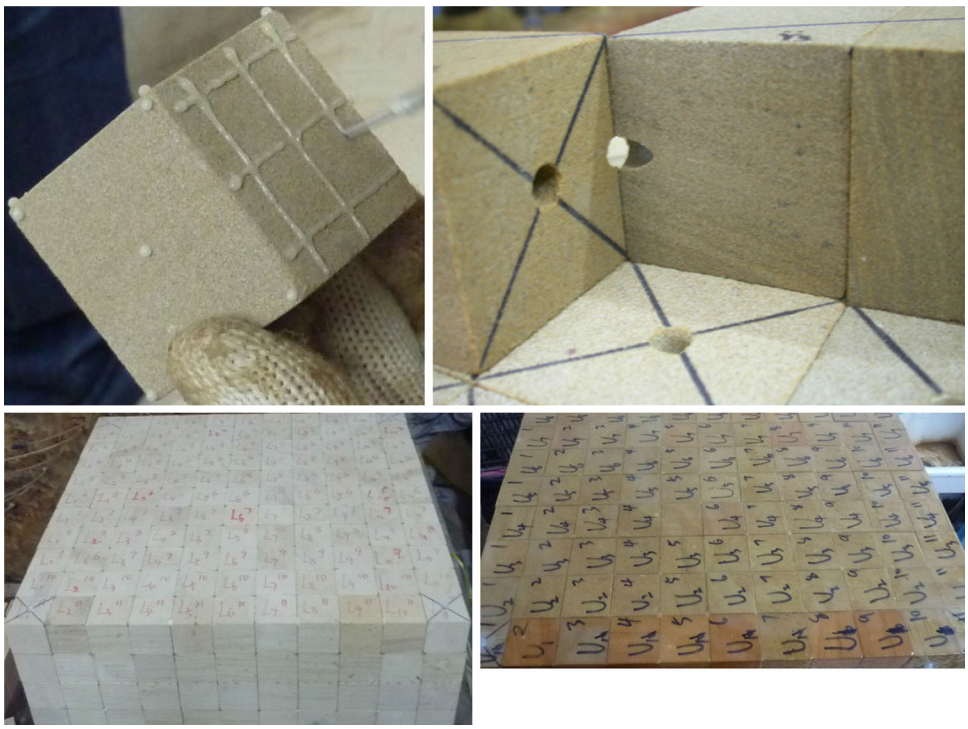

Fig. 5 Manufacture process for experimental model

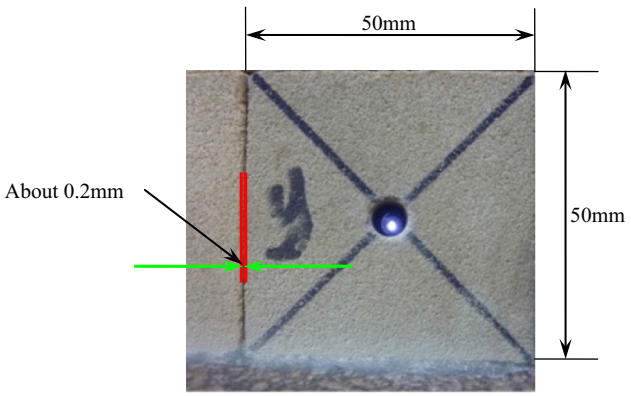

Fig. 6 Structure of dual porous media

Fig. 7 Experimental model

permeability model. The parameters of numerical model and experimental model, such as the size and properties, are all the same. The gridding number is $11 \times 11 \times 42 = 5{,}042$. In vertical direction, the 1st to 21st are the matrix systems, the 22nd to 42nd are the fracture systems, and the gridding size are 5 cm × 5 cm × 5 cm. Therefore, the experimental model established method could be verified by the software based on experimental data matching.

1. Permeability of fracture is much greater than that of matrix. Under the experimental pressure, fluid flow through the reservoir takes place only in the fracture network with the matrix blocks acting as sources. This is regarded as a dual porosity single permeability system, so dual porosity single permeability model is chosen in numerical model.
2. In water-wet fractured reservoirs, the matrix rock has a positive water–oil capillary pressure. After water is introduced into the fracture, the water flows under capillary forces into the matrix system to displace oil. Therefore, imbibition between matrix and fracture should be consid-

Table 3 Parameters of target reservoir and experimental model

Parameters	Field	Model	Notes
Size	250 m × 250 m × 500 m	0.55 m × 0.55 m × 1.05 m	$\pi_1-\pi_5$
Well radius (m)	0.14	0.06	π_6
Fracture permeability in x direction (mD)	121.18	3,836	$\pi_7-\pi_{11}$
Fracture permeability in y direction (mD)	127.24	4,027	
Fracture permeability in z direction (mD)	169.65	5,370	
Matrix porosity (%)	2.84	16	π_{12}
Fracture porosity (%)	0.72	1.0	
Matrix irreducible water saturation (%)	47.8	54.2	$\pi_{13}-\pi_{22}$
Matrix residual oil saturation (%)	30	21.8	
Movable oil ratio of matrix and fracture	1.3:1	1.3:1	
Oil viscosity (mPa s)	7.72	14.48	
Water viscosity (mPa s)	0.533	1	
Oil–water viscosity ratio	14.48	14.48	
Water density (g/cm^3)	1	1	
Oil density (g/cm^3)	0.82	0.915	
Water–oil density difference (g/cm^3)	0.18	0.085	
Injection–production pressure	16 MPa	0.27 m water column	

Table 4 Compositions of injected water

Ion	Concentration (mg/L)	Ion	Concentration (mg/L)
$K^+ + Na^+$	782.69	SO_4^{2-}	9.61
Ca^{2+}	8.02	HCO_3^-	1,452.58
Mg^{2+}	2.43	CO_3^{2-}	95.22
Cl^-	327.93	Salinity	2,678.48

ered, while the fracture cells usually have zero capillary pressure.

Wettability is reflected by oil–water relative permeability curve. In the reservoir, the minimum saturation of wetting phase is greater than that of non-wetting phase; the relative permeability of non-wetting phase increases with its saturation faster than wetting phase. Therefore, the reservoir wettability of numerical model can be determined by the characteristics of the relative permeability curve. Because the reservoir is hydrophilic reservoir, a hydrophilic relative permeability curve is adopted in numerical model as shown in Fig. 8. Relative permeability curve of fracture system is shown in Fig. 9.

3. Due to its great thickness of buried hill reservoirs, fluid gravity must be considered.
4. The fracture permeability of actual reservoir is anisotropic; therefore, the fracture permeability of the experimental model and numerical models is anisotropic.
5. Compressibility of the fluid and rock is ignored due to tiny pressure fluctuation range, when well pattern variation is the only factor to be considered.

Compared the experimental results with the numerical simulation, we find that the experiments are closer to that of the numerical simulation, which indicates the reliability of the experimental method.

5.2 Macroscopic Development Law

5.2.1 Liquid Rate

Figure 10 indicates that under a pressure difference of 0.27 m water column, the liquid rate of Case 2 is the highest, followed by Case 3, with that of Case 1 being the lowest.

The reason for the difference in liquid rate lies in the different drilling ratios of fractures for different well types. The liquid rate of the vertical well is the lowest because of the lowest drilling ratio of fractures in a buried hill reservoir, in which mid–high-angle fractures developed as dominant channels for oil–water migration. By contrast, the ratio of drilling through fractures, as well as the drainage volume of horizontal wells, is relatively higher under lower injection–production pressure difference. The controlling area and drilling ratio of fishbone wells are even larger because of the branch, which shortens the distance between the injection and production wells, resulting in an increasing pressure gradient.

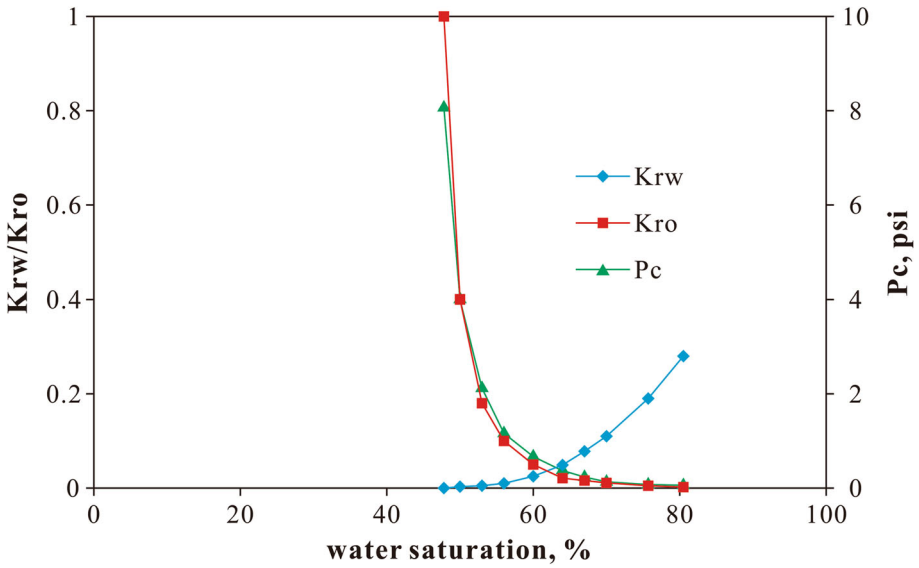

Fig. 8 Relative permeability curve of matrix and capillary pressure

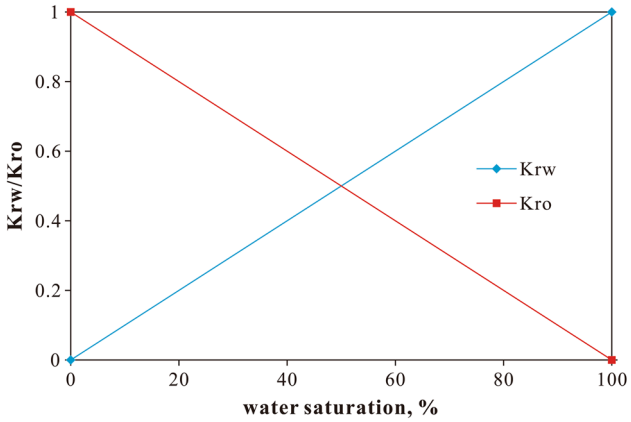

Fig. 9 Relative permeability curve of fracture

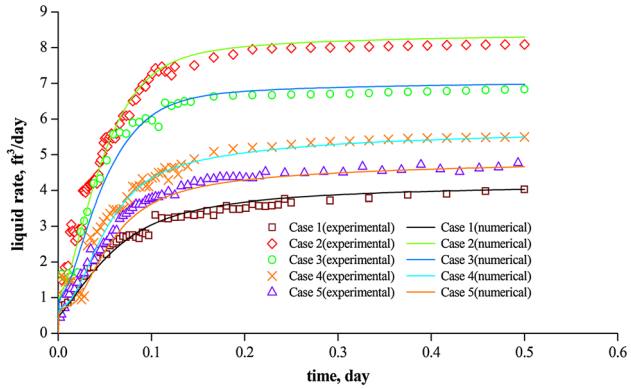

Fig. 10 Variations of liquid production by different well patterns

5.2.2 Water Cut

In Fig. 11, Case 1 features the fastest water breakthrough and most rapid increase in water cut, followed by Cases 2, 3, and 4, with that of Case 5 being the slowest.

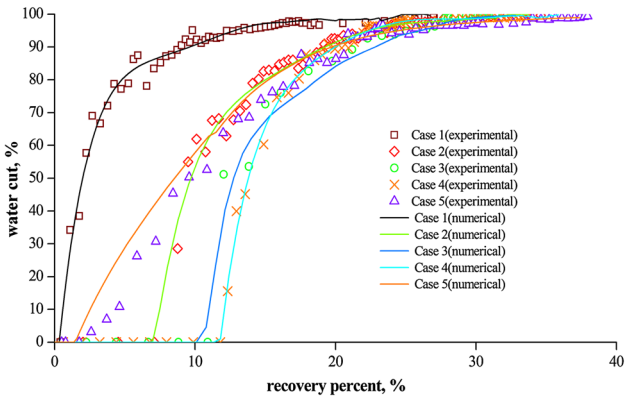

Fig. 11 Variations of water cut with recovery by different well patterns

For Case 1, the oil–water front breaks through along the bottom plane of the reservoir, whereas in the other cases, which involve the stereo injection–production of complex structure wells, the oil–water fronts are restrained by gravity, which prolongs the water–free oil production period. The branches of the fishbone well expand the injection area, causing injected water to migrate gently. Once water breakthrough occurs in the fishbone well, the water cut will increase more rapidly than that in horizontal wells.

5.2.3 Oil Recovery Percentage

The oil recovery percentage of water–free oil production period from highest to lowest is in the order of Case 4, 3, 2, 5, and 1, with oil recoveries of 11.8, 10.9, 7.1, 2.6, and 1.1 %, respectively. The final oil recoveries are 33.93, 31.40, 34.60, 37.94, and 27.48 %. The results show that the vertical well features the lowest oil recovery. Compared with vertical wells, complex structure wells have larger areas of con-

tact with the reservoir and a higher ratio of drilling through fractures, which contribute to the development advantages. Fishbone wells tend to make the oil–water front gentler when the percolation direction is perpendicular to the plane determined by the mother bore and its branch, which induces gentle water coning. Therefore, by making the plane determined by the mother bore and its branch vertical to the percolation direction, satisfactory development can be achieved by using a fishbone well.

6 Conclusions

- The method for the establishment of the experimental model and wellbore presetting are proposed according to discretization. Different well patterns can be realized by selectively plugging different wells in the model.
- Combined with target reservoir, the similarity experimental model is designed and fabricated according to the water flooding similarity principle of a fractured reservoir, which fully accords with similarity, such that the development process of a fractured reservoir can be simulated.
- Numerical model is established which the parameters are the same with experimental model. And reliability of the experimental model establishing method is verified by the software based on experimental data matching.
- The results of experiments and numerical simulation illustrate that complex structure well patterns can contribute to higher oil recovery compared with vertical well patterns in buried hill reservoirs. Considering the experimental index (liquid rate, water cut, and oil recovery), the horizontal–horizontal well pattern is recommended.
- For fishbone wells, if the plane determined by the mother bore and its branch is vertical to the percolation direction, the oil–water front will be gentle, and injected water will cone gently.

Acknowledgments The authors would like to express their appreciation for the financial support received from Nation Natural Science Foundation of China (No. 51374222) and National Science and Technology Major Project "Complicated oil and gas geology and EOR Technology" (No. 2011ZX05009-004-001).

References

1. Delamaide, E.; Renard, G.; Kalaydjian, F.; Lobey, O.; Duquerroix, J.P.: How to choose the best tool in the new toolbox of reservoir engineers: complex structure well architectures. In: SPE international conference on horizontal well technology held in Calgary, Canada, SPE 37083, 18–20 Nov 1996
2. Xing, G.Y.; Guo, F.X.; Song, C.; Sun, Y.C.; Yu, J.; Wang, G.: Fishbone well drilling and completion technology in ultra-thin reservoir. In: IADC/SPE Asia Pacific drilling technology conference and exhibition held in Tianjin, China, IADC/SPE 155958, 9–11 July 2012
3. Cuadros, J.; Ossa, N.; Cuadros, G.; Rojas, E.: Horizontal well placement optimization for heavy oil production in girasol field. In: The Trinidad and Tobago energy resources conference held in Port of Spain, Trinidad, SPE 132884, 27–30 June 2010
4. John, L.S.; Gregory, D.Y.; Robert, J.K.; Carl, M.; Tony, L.; Petrozuata, C.A., Jeffery H.: Multilateral-horizontal wells increase rate and lower cost per barrel in the Zuata field; Faja; Venezuela. In: SPE international thermal operations and heavy oil symposium held in Porlamar, Margarita Island, Venezuela, SPE 69700, 12–14 March 2001
5. Raghavan, R.; Joshi, S.D.: Productivity of multiple drainholes or fractured horizontal wells. In: SPE Eastern regional meeting held in Columbus, OH, SPE 21263, Oct 31–Nov 2 1990
6. Larsen, L.: Productivity computations for multilateral; branched; and other generalized and extended well concepts. In: SPE annual technical conferences and exhibition held in Denver, USA, SPE 36754, 6–9 Oct 1996
7. Fan, Y.P.; Han, G.Q.; Yang, C.C.: Production forecast for herringbone well and optimum configuration of lateral holes. Acta Pet. Sin. **27**(4), 101–104 (2006)
8. Guo, B.; Sun, K.; Ghalambor, A.: Well Productivity Hand Book. pp. 226–230. Gulf Publishing Company, Houston, TX (2008)
9. Yang, X.S.; Liu, C.X.; Yan, J.; Wang, W.H; Shi, Z.L.; Jia, Y.: Research on productivity law of herringbone multilateral gas well. Acta Pet. Sin. **29**(5), 727–733 (2008)
10. Jamil, A.T.; Shamsuddin, S.; Bevan, Y.: Simulation optimization of wells with complex architecture. In: Offshore technology conference held in Houston, Texas, USA, OTC 20131, 4–7 May 2009
11. Crumpton, P.I.; Habiballah, W.A.; Wardell-Yerburgh, P.G.; Nasser, K.A.; Faleh, A.A.: Multilateral-complex structure well optimization. In: SPE reservoir simulation symposium held in The Woodlands, Texas, USA, SPE 140882, 21–23 Feb 2011
12. Zhang, S.M.; Zhou, Y.J.; Song, Y.; Wan, H.Y.; An, Y.S.; Xu, Q.; Dong, Z.G.: Design optimization for the horizontal well pattern with herringbone-like laterals. Pet. Explor. Dev. **38**(5), 606–612 (2011)
13. Jiang, H.F.; Sui, J.; Pang, Y.M.; Zhang, G.L.; Liu, Y.T.: Technique of exceptionally low abundance oil reservoir development by horizontal wells and its application. Pet. Explor. Dev. **33**(3), 364–368 (2006)
14. Al-Muntasheri, G.A.: Conformance control with polymer gels: what it takes to be successful. Arab. J. Sci. Eng. **37**(4), 1131–1141 (2012)
15. Kader, A.K.A.; Kordik, P.; Khalil, A.; Mekkawi, M.; El-Bohoty, M.; Rabeh, T.; Refai, M.K.; El-Mahdy, A.: Interpretation of geophysical data at EL Fayoum—Dahshour Area, Egypt using three dimensional models. Arab. J. Sci. Eng. **38**(7), 1769–1784 (2013)
16. Zhou, H.M.; Chang, X.J.; Hao, J.M.; Zheng, J.M.: Horizontal well development technique and its practice for complex fault-block reservoirs in Jidong oilfield. Pet. Explor. Dev. **33**(5), 622–629 (2006)
17. Zhou, Y.J.: Advances on special structure drilling development techniques in Shengli oilfield. Pet. Explor. Dev. **35**(3), 318–329 (2008)
18. Hao, M.Q.; Hu, Y.L.; Liu, X.; Wei, C.J.; Zhuang, Y.T.: Predicting and optimizing the productivity of multiple transverse fractured horizontal wells in ultra-low permeability reservoirs. IPTC; 16891 (2013)

19. Yu, X.C.; Guo, B.Y.; Ai, C.; Bu, Z.D.: A comparison between multi-fractured horizontal and fishbone wells for development of low-permeability fields. In: SPE Asia Pacific oil and gas conference and exhibition held in Jakarta, Indonesia, SPE 120579, 4–6 Aug 2009
20. Bigno, Y.; Al-Bahry, A.; Melanson, D.D.; Al-Hasani, S.; Senger, J.C.; Henning, R.: Multilateral waterflood development of a low-permeability carbonate reservoir. In: SPE annual technical conference and exhibition held in New Orleans, Louisiana, SPE 71609, 30 Sept–3 Oct 2001
21. Zhou D.; Jiang T.; Feng J.; Bian W.; Liu Y.: Research of water flooded performance and pattern in horizontal well with bottom-water drive reservoir. In: The petroleum society's 5th Canadian international petroleum conference (55th annual technical meeting), Calgary, Alberta, Canada, PETSOC 2004-093, 8–10 June 2004
22. Fipke, S.; Celli, A.: The use of multilateral well designs for improved recovery in heavy-oil reservoirs. In: IADC/SPE drilling conference held in Orlando, Florida, USA, SPE 112638, 4–6 March 2008
23. Liu, X.P.; Zhang, Z.S.; Cui, G.X.; Wang, J.L.; Yi, F.X.: Inflow performance relationship of a herringbone multilateral well. Acta Pet. Sin. **21**(6), 57–60 (2000)
24. Yan, P.; Medhat, M.K.; Jitendra, K.: Applications of a semianalytical model of multilateral wells in multilayer reservoirs. In: SPE western regional meeting held in San Jose, California, USA, SPE 121335, 24–26 March 2009
25. Maricic, N.; Mohaghegh, S.D.; Artun, E.: A parametric study on the benefits of drilling horizontal and multilateral wells in coalbed methane reservoirs. In: SPE annual technical conference and exhibition held in Dallas, Texas, SPE 96018, 9–12 Oct 2005
26. Nestor, R.; Amit, K.; Arun, K.; Younes, J.: Application of multilateral wells in solution gas-drive reservoirs. In: SPE international petroleum conference and exhibition in Mexico held in Villahermosa, Mexico, SPE 74377, 10-12 Feb 2002
27. Zimmerle, W.: Petroleum Sedimentology. Kluwer Academic Publishers, Dordrecht (1995)
28. Lei, Y.; Chen, Y.; Shang, X.F.; Chen, Z.G.; Wu, S.; Zhao, Y.; Liu, Y.Q.: Application of multilateral wells in burial-hill migmatitic granite formation. In: IADC/SPE Asia Pacific drilling technology conference and exhibition held in Tianjin, China, IADC/SPE 155700, 9–11 July 2012
29. Xie, W.Y.; Meng, W.G.; Zhang, Z.W.; Li, X.G.; Chen, Z.Y.: Formation model of multi-stage fracture reservoirs inside the buried hills in Liaohe depression. Pet. Explor. Dev. **33**(6), 649–652 (2006)
30. Ding, Z.P.; Liu, Y.T.; Zhang, Y.; Ao, K.: A quantitative 3D physical simulation method of waterflooding in fractured reservoirs. Pet. Sci. Technol. **30**(12), 1250–1261 (2012)
31. Ding, Z.P.; Liu, Y.T.; Gong, Y.J.; Xu, N.: A new technique: fishbone well injection. Pet. Sci. Technol. **30**(23), 2488–2493 (2012)
32. Ren, F.X.: Discussions on tridimensional reservoir development models. Pet. Explor. Dev. **39**(3), 320–325 (2012)
33. Ding, Z.P.; Liu, Y.T.; Luo, Y.Y.; Ao, K.: Optimization design of horizontal well stereo injection and production in buried hill reservoirs. Well Test. **20**(2), 49–51 (2011)
34. Zhao, L.X.; Jiang, M.H.; Zhao, X.F. et al.: Research on deliverability relationship of complicated horizontal well. J. Univ. Pet. China (Edition of Natural Science) **30**(3), 77–80 (2006)
35. Wang, X.D.; Yu, G.D.; Li, Z.P.: Productivity of horizontal wells with complex branches. Pet. Explor. Dev. **33**(6), 729–733 (2006)
36. Liu, Y.T.; Ding, Z.P.; Ao, K.; Zhang, Y.; Wei, J.: Manufacturing method of large-scale fractured porous media for experimental reservoir simulation. SPE J., 163108-PA (2013)
37. Liu, Y.T.; Ding, Z.P.; Qu, Y.G.; Zhao, C.J.: The characterization of fracture orientation and the calculation of anisotropic permeability parameters of reservoirs. Acta Pet. Sin. **32**(5), 842–846 (2011)